Error-signaling in the developing brain

Mary Abbe Roe[a,*], **Laura E. Engelhardt**[a], **Tehila Nugiel**[a], **K. Paige Harden**[a,b], **Elliot M. Tucker-Drob**[a,b], **Jessica A. Church**[a,c]

[a]Department of Psychology, The University of Texas at Austin, Austin, TX, United States

[b]Population Research Center, The University of Texas at Austin, Austin, TX, United States

[c]Biomedical Imaging Center, The University of Texas at Austin, Austin, TX, United States

Abstract

While learning from mistakes is a lifelong process, the rate at which an individual makes errors on any given task decreases through late adolescence. Previous fMRI adult work indicates that several control brain networks are reliably active when participants make errors across multiple tasks. Less is known about the consistency and localization of error processing in the child brain because previous research has used single tasks. The current analysis pooled data across three studies to examine error-related task activation (two tasks per study, three tasks in total) for a group of 232 children aged 8–17 years. We found that, consistent with the adult literature, the majority of applied cingulo-opercular brain regions, including medial superior frontal cortex, dorsal anterior cingulate, and bilateral anterior insula, showed consistent error processing engagement in children across multiple tasks. Error-related activity in many of these cingulo-opercular regions correlated with task performance. However, unlike in the adult literature, we found a lack of error-related activation across tasks in dorsolateral frontal areas, and we also did not find any task-consistent relations with age in these regions. Our findings suggest that the task-general error processing signal in the developing brain is fairly robust and similar to adults, with the exception of lateral frontal cortex.

Keywords

Child; Control; fMRI; Mistakes; Executive function; Reading

---

*Corresponding author at: Department of Psychology, The University of Texas at Austin, 108 E. Dean Keeton Stop A8000, Austin, TX 78712-1043, United States. maroe@utexas.edu (M.A. Roe).

1. Introduction

Learning from one's mistakes is important for social development, academic performance, and occupational success. A key marker of adaptative behavior and learning is error reduction over time. In development, errors typically decrease through late adolescence, and this is thought to reflect the maturation of cognitive abilities that support goal-directed behaviors and error processing (Fitzgerald et al., 2010; Luna et al., 2010; Rubia et al., 2006; Velanova et al., 2008). Disorders characterized by poor behavioral regulation of control that emerge during childhood and adolescence (e.g., attention-deficit/hyperactivity disorder; Kessler et al., 2007; Merikangas et al., 2010) often relate to greater production of mistakes or an inability to improve performance after an error (Carrasco et al., 2013; Johnson et al., 2007; Mullane et al., 2009; Plessen et al., 2016; Schachar et al., 2004).

Cognitive theories of error processing consider errors as a type of unexpected event that lead to processes that either improve or reduce behavioral accuracy on the task (Wessel and Aron, 2017). Most of the neural support for these theories comes from temporally-powerful techniques like electroencephalography (EEG), which can measure event-related brain potentials during and after errors (ERPs; for a review see Tamnes et al., 2013). The error-related negativity (ERN) component, which is a negative deflection of the ERP that occurs after an individual makes an error, is thought to originate, in part, from the anterior cingulate cortex (ACC) and its functional network, regardless of the type of task (Holroyd and Coles, 2002). Consistent with, and expanding on ERN work, recent adult studies investigating error-related brain activation that use the more spatially specific method of functional magnetic resonance imaging (fMRI) find that the error-signaling mechanism in the adult brain involves the ACC and a large set of additional putative control regions (Neta et al., 2015).

The error fMRI brain signal is measured by directly comparing activation during error trials (incorrect and omitted responses) to activation during correct trials, and is generally marked by more positive activation for errors relative to correct trials. A meta-analytic examination of fMRI studies of healthy adults has identified a set of error-related brain regions that consistently show this pattern across a wide variety of tasks (Neta et al., 2015). However, researchers have not yet investigated error signaling in a large sample of children across multiple tasks to identify whether consistent error-related activation in children is spatially similar to brain regions found in adults. Identifying a set of error-related brain regions during typical development builds a framework for understanding aberrant error processing in populations at risk of developing control-related disorders (Kessler et al., 2007; Merikangas et al., 2010).

Error-related brain regions in adults are spread across multiple areas within the frontal, parietal, and occipital cortical lobes, in addition to subcortical and cerebellar regions (Neta et al., 2015). These regions are purported to be critical for control-demanding tasks (e.g., reading, making judgements about images or abstract concepts, flexibly adjusting to rules; Dosenbach et al., 2006; Engelhardt et al., 2019), and these regions also correlate together in their resting blood-oxygen-level dependent (BOLD) signal, even in the absence of a task (Dosenbach et al., 2008, 2006; Neta et al., 2015, 2014; Power and Petersen, 2013). Many of

these error-related regions are within the brain's fronto-parietal and cingulo-opercular putative control networks, indicative of a clear role for control in error processing and task performance (Neta et al., 2015).

Developmental studies of single-task fMRI (Braet et al., 2009; Deng et al., 2017; Fitzgerald et al., 2010, 2008; Rodehacke et al., 2014; Rubia et al., 2007; Stevens et al., 2009) and electroencephalography (Tamnes et al., 2013) have indicated that at least some of these control regions are indeed engaged during errors relative to correct trials in childhood. These studies most often find greater engagement of cinguloopercular regions like the dorsal anterior cingulate (dACC) and anterior insula, with additional regions differing across studies (Braet et al., 2009; Deng et al., 2017; Fitzgerald et al., 2010, 2008; Rodehacke et al., 2014; Rubia et al., 2007; Stevens et al., 2009). For example, some studies have found that children show adult-like error activation in control regions like the inferior parietal lobule (Braet et al., 2009; Stevens et al., 2009), while others have reported age-related differences in the lingual gyrus and caudate (Braet et al., 2009; Fitzgerald et al., 2010; Rubia et al., 2007). Overall, reports of fronto-parietal control engagement during errors, especially in the lateral frontal lobes, are inconsistent across single-task child fMRI studies (Braet et al., 2009; Deng et al., 2017; Fitzgerald et al., 2010, 2008; Rodehacke et al., 2014; Rubia et al., 2007; Stevens et al., 2009).

A multiple-fMRI-task approach that also examines relations between age, accuracy, and activation may clarify whether fronto-parietal control regions differentiate mature from immature error processing in children. Individuals make errors during many different types of control-demanding tasks (Neta et al., 2015), yet all of the single-task developmental fMRI studies have investigated error activation solely in the context of inhibitory control (Braet et al., 2009; Deng et al., 2017; Fitzgerald et al., 2010, 2008; Rodehacke et al., 2014; Rubia et al., 2007; Stevens et al., 2009). These tasks are designed to tap regulatory cognitive processes that require participants to inhibit learned or dominant motor responses. Inhibitory control tasks are useful for producing high error rates to examine error-related activation, but may limit the scope of our understanding of error processing in the developing brain if the regions engaged for errors during inhibition are not common across a wide array of tasks. Further, a multi-task approach has been helpful in studying functional brain network consistencies in children for *correct* task performance (Engelhardt et al., 2019), and thus a similar approach could be utilized to inform our understanding of error processing in children.

The goal of the current study was to identify brain regions that respond differentially to errors and correct trials in typically developing children across three different tasks, and to compare error regions identified in these pediatric samples to literature-derived adult error regions. The three tasks included a reading comprehension task (making judgements about the sensibility of sentences), an inhibition task (inhibiting learned responses), and a cognitive flexibility task (cued switching between rules when sorting shapes). First, we applied the same approach used by adult (Neta et al., 2015) and child (Engelhardt et al., 2019) meta-analyses to identify clusters of error-related brain activity common across the 3 tasks, pooling fMRI data from over 200 children ages 8 to 17 years. Second, we estimated the distance between the neuroanatomical locations of the observed child error regions and

adult error regions (Neta et al., 2015) to determine whether the spatial organization of regions critical for error processing in children was similar to that of adults. Finally, we tested the extent to which task accuracy or age explained some variability in error-related brain activation by correlating it with activation across the entire child sample. We predicted that children would have a similar set of consistent cingulo-opercular error-related regions to adults, and that greater engagement of error regions would relate to better task performance. Our review of the single-task fMRI literature for error processing in children suggests a lack of consistent lateral frontal cortex activity. Therefore, we leveraged the multiple-task approach to test whether engagement in the frontal aspects of the fronto-parietal control network would be more task specific or more consistent across multiple tasks in our sample.

2. Materials and methods

2.1. Studies and participants

Data in this analysis included three tasks collected for three separate studies: an Executive Function Study ($N = 28$), a Twin Study ($N = 77$), and a Reading Study ($N = 127$; total $N = 232$). Participants were aged 8–17 years ($M = 10.60$ years, $SD = 1.56$ years, 51% female; Table 1) and had no reported diagnoses of psychiatric or developmental disorders. Parents provided written informed consent for their child's participation, and participants provided written informed assent. Participants were compensated for their time. The Institutional Review Board of the University of Texas at Austin approved the Executive Function and Twin studies, and the Institutional Review Board of the University of Texas Health Science Center at Houston approved the Reading study for the Austin and Houston sites.

For the Twin and Reading Studies, the participants included in our analyses differed slightly from the participants included in previously published studies. For both studies, we excluded participants who had perfect performance on a task, given that we could not use them to examine error trial activation. For the Twin study sample, we analyzed data from one twin randomly selected from each twin pair, originally collected as part of the Texas Twin Project (Engelhardt et al., 2019; Harden et al., 2013). For the Reading Study (Nugiel et al., 2019; Roe et al., 2018), we lowered the performance criteria to allow for greater variability in performance and to have consistent criteria across the three studies used here. We also excluded any participants from the original Reading Study sample that had clinical diagnoses of dyslexia or attention-deficit/hyperactivity disorder; our Reading Study sample here included some participants who were labeled as struggling readers by scoring below a cutoff on school administered reading tests. The Executive Function Study design was the same as the Twin Study, but focused collection on a sample of children with and without control-related disorders; we analyzed only the typically developing sample that passed performance and movement criteria for the current study.

All studies were conducted at The University of Texas at Austin Biomedical Imaging Center ($N = 193$), with the exception of a subset of the Reading Study participants ($N = 39$) collected at The University of Texas Health Science Center at Houston (see MRI data acquisitions across studies). Group-level fMRI analyses showed no significant differences between sites for the reading and inhibition task error contrasts, allowing for collapse across collection sites for these tasks.

Following the adult error meta-analysis by Neta and colleagues (Neta et al., 2015), error trials were modeled separately from correct trials, errors of both commission and omission were examined together, and all of the tasks were absent of any explicit feedback. Due to the nature of the original goals of each study, the tasks were all visually presented and had a button-press response. Participants were asked to make judgements about the sensibility of sentences, to inhibit learned responses, and to switch between rules when matching shapes (see fMRI tasks).

2.2. MRI data acquisitions across studies

All scan sessions included high-resolution structural (T1 and T2) and DTI scans, in addition to resting state and task-related fMRI scans. The Twin and Executive Function Studies included two in-scanner tasks reported here: the inhibition task (1 run per Twin Study participant and 1–2 runs per Executive Function Study participant) and the flexibility task (1–2 runs per participant for both studies; see Table 2 and Supplementary Fig. 1 for task designs). At both the Austin and Houston Reading study imaging sites, the two in-scanner tasks were the inhibition (1–2 runs per participant) and the reading tasks (1–3 runs per participant). Before performing tasks inside the scanner, participants practiced each task on a computer outside the scanner room, and were reminded of task instructions prior to each task collection. All MRI sessions lasted approximately 90 min.

2.2.1. Twin, executive function, and Austin reading studies (N = 193)—Images
were acquired on a Siemens Skyra 3-Tesla scanner with a 32-channel head matrix coil at the University of Texas at Austin Biomedical Imaging Center. T1-weighted structural images were collected with an MPRAGE sequence (TR = 2530 ms, TE = 3.37 ms, FOV = 256, $1 \times 1 \times 1$mm voxels), and T2-weighted structural images were collected with a turbo spin echo sequence (TR = 3200 ms, TE = 412 ms, FOV = 250, $1 \times 1 \times 1$ mm voxels). Task functional images were collected using a multi-band echo-planar sequence (TR = 2000 ms, TE = 30 ms, flip angle = 60°, multiband factor = 2, 48 axial slices, $2 \times 2 \times 2$ mm voxels, base resolution = 128×128). All tasks were run using PsychoPy software (Peirce, 2007) and stimuli were projected onto a screen (resolution of 1920×1080) that participants viewed using a mirror attached to the head coil. Participants used Optoacoustics headphones (OptoAC-TIVE Optical MRI Communication System with Active Noise Control) and responded using a two-button response box (FIU-932 Current Designs).

2.2.2. Houston reading study (N = 39)—The Houston site MRI data were acquired
with a Siemens TIM Trio Syngo 3T MRI scanner with a 12-channel head coil at the Baylor Imaging Center. Isotropic 3D T_1-weighted structural images were acquired in the sagittal plane (TR = 2170 ms, TE = 3.6 ms, FOV = 256, $1 \times 1 \times 1$ mm voxels, flip angle = 7°, NEX = 1, iPAT = 3) and a turbo-spin echo sequence to collect T_2-weighted structural images (TR = 3200 ms, TE = 410 ms, FOV = 256, $1 \times 1 \times 1$ mm voxels). Isotropic 2D functional images for both tasks were acquired in the axial plane (TR = 2000 ms, TE = 30 ms, flip angle = 79°, 32 axial slices, $3 \times 3 \times 3$ mm voxels, base resolution = 96×96, NEX = 1, iPAT = 3). Stimuli at the Houston site were presented on a Cambridge Research Systems BOLDscreen 32 LCD monitor projector at the same resolution as the University of Texas at Austin Biomedical

Imaging Center site. Houston participants used the same Optoacoustics headphones and FIU-932 Current Designs button box controller.

2.3. fMRI tasks

2.3.1. Inhibition task—For inhibition we used the Stop Signal Task, adapted from Verbruggen and Logan (Verbruggen and Logan, 2008), where participants were instructed to respond to arrows pointing left or right on the screen ("Go" trials), but to not respond if a red X appeared on top of the arrow ("Stop" trials; Supplementary Fig. 1). Each run consisted of 96 "Go" trials and 32 "Stop" trials (25% of the trials). The current study analyzed "Stop" trials only for brain activation, using the error contrast *correct stops vs. failed stops*, in order to focus on the task's main interest of inhibitory control. A "Stop" trial started with the presentation of a left- or right-pointing arrow in the center of the screen for 250 ms (the initial Stop Signal Delay, SSD), then the "Stop" signal (a red X) overlapped the arrow; the "Stop" signal remained on the screen for the duration of that trial (1000 ms). If a participant correctly inhibited a button response during the first "Stop" trial, the SSD for the next "Stop" trial increased 50 ms (SSD to 300 ms). If a participant incorrectly made a button response during a stop trial, then the SSD decreased by 50 ms on the next "Stop" trial (SSD to 200 ms); this staircasing continued throughout each run of the inhibition task, driving participants towards a 50% stop rate (Verbruggen and Logan, 2008). A "Go" trial consisted of a left- or right- pointing arrow in the center of the screen presented for 1000 ms. Each trial type was followed by 1000 ms of blank screen (inter-stimulus interval) and interspersed with a jittered blank screen ranging from 0–7000 ms. The inhibition task runs lasted 6'0" with 180 frames each.

2.3.2. Flexibility task—Participants were instructed to pay attention to the shape or color (rules) of a target stimulus that would later appear after the cue period (Supplementary Fig. 1; Engelhardt et al., 2019). The two possible rules and two responses choices were displayed on the screen for the entire length of the trial (4000 ms). For the first 1500 ms of the trial, a red box indicated which rule to follow (cue period). The flexibility task runs consisted of 46 trials; for 37 of the 46 trials, the target stimulus appeared 500 ms after the red box disappeared and then the target remained on the screen for 2000 ms (response period). During the response period, the participant could indicate which of the response choices matched the target. A 1000 ms fixation cross followed the response period and a jittered blank screen of 0–8000 ms followed all trials. In 9 cue-only trials interspersed throughout the run, a red fixation cross was displayed for 500 ms instead of a target, which was then followed by a white fixation cross for 500 ms. The flexibility runs were administered up to two times per participant. During the first run, there were 22 repeat trials where the cued rule was consistent with the rule on the previous trial. The repeat trials were interspersed with 23 switch trials where the cued rule switched. During the second run, there were 23 repeat trials and 22 switch trials. For maximal power of error trials, the current study collapsed across switch and repeat trials, using the contrast *all correct trials vs. all error trials*. The flexibility task runs lasted 5'22" with 161 frames each.

2.3.3. Reading task—The reading task was closely adapted from Meyler and colleagues (Meyler et al., 2007) for the purposes of specific questions for the Reading Study (Nugiel et

al., 2019; Roe et al., 2018). Participants indicated if short sentences were sensible or non-sensible and were not provided with performance feedback (Supplementary Fig. 1); for the current analysis, we collapsed across sensibility-type to examine the error contrast *all correct vs. all error*. The task was administered up to three times; each run started with the probe "Makes Sense?" for 2000 ms, followed by 32 sentence trials. The sentences were presented for 8000 ms followed by 2000 ms of blank screen (inter-stimulus interval) and interspersed with a jittered blank screen ranging from 0–8000 ms. Participants used their thumbs to press buttons on a button box that indicated the sensibility of the sentence. The words "No" and "Yes" appeared in small font below the sentence on either side of the screen to remind the participant of the response mapping onto the buttons (left/right), which was counter-balanced across participants. The reading task runs lasted 7'6" with 212 frames each.

2.4. Analyses

2.4.1. Behavioral analyses—Analyses of behavioral performance were conducted in *R* version 3.3.3 (R Development Core Team, 2017). Performance criteria were selected to allow as much variability in task performance as possible, while ensuring that participants engaged in the task. Runs were excluded if performance did not meet the following criteria: for inhibition, "Go" accuracy on greater than 50% of "Go" trials and Stop Signal Reaction Time (SSRT) greater than 50 ms (Congdon et al., 2012); for flexibility, at least 50% accuracy; for reading, at least 50% accuracy. SSRT estimates were calculated using the quantile method, which subtracts the mean SSD from the quantile RT (the RT for the correct "Go" trials that corresponds to the proportion of failed inhibition; Congdon et al., 2012). For the Executive Function Study, 92% of participants had two inhibition and two flexibility task runs. Participants in the Twin Study all had one inhibition task run, and 79% had two flexibility task runs. For the Reading Study, 94% of participants had two inhibition task runs and 89% of participants had two to three reading task runs (see Supplementary Notes: Participant Characteristics for details). Task performance was averaged across usable runs.

2.4.2. fMRI preprocessing—Imaging data from the Twin Study (Engelhardt et al., 2019) and Executive Function Study were preprocessed with the fMRI Expert Analysis Tool in FMRIB Software Library (FSL) version 5.0.9 (www.fmrib.ox.ac.uk/fsl). Imaging data acquired for the Reading Study (Nugiel et al., 2019; Roe et al., 2018) were preprocessed with FSL version 5.0.2 for original analyses published in Roe and colleagues (Roe et al., 2018). We were able to add 13 participants to these new analyses due to inclusion criteria differences between this study and Roe and colleagues (Roe et al., 2018); the first and second-level analyses for these additional 13 Reading Study participants were processed using FSL version 5.0.9 due to unavailability of the older FSL 5.0.2 software on our supercomputer. All participant data was reviewed for alignment and preprocessing quality.

High-resolution T1-weighted structural images from all studies, regardless of FSL version, underwent skull stripping and brain extraction using Freesurfer version 5.3.0 (Reuter et al., 2010). Functional data were registered to the structural image using the Boundary-Based Registration algorithm (Greve and Fischl, 2009), and structural images were registered to MNI space using the FMRIB Linear Image Registration Tool (Jenkinson et al., 2002; Jenkinson and Smith, 2001). Pre-statistics processing also included spatial smoothing using

a Gaussian kernel of FWHM 5mm, grand-mean intensity normalization of the 4D dataset by a single multiplicative factor, and high pass temporal filtering (Gaussian-weighted least-squares straight line fitting, with 50 s sigma).

2.4.3. fMRI analyses—We analyzed the following error contrasts from each task: *correct stops vs. failed stops* for the inhibition task; *all correct vs. all error trials*, which combined across both cue and target periods per trial, for the flexibility task; *all correct vs. all error trials* for the reading task. For a single task, the recommended minimum number of error trials necessary to detect a reliable error-related signal for sample sizes greater than 90 is two trials (Steele et al., 2016). For all of our tasks, therefore, we included participants with usable data that had at least two error trials, with the exception of inclusion of four participants for the flexibility task with one error trial, in order to maximize our total sample size for that task (total flexibility task $N = 95$), and because the flexibility results held without these four participants. Of note, because the SSD of the inhibition task used staircasing to guide stop accuracy to about 50%, the number of errors in that task are highly consistent across individuals, unlike the more traditional designs of the flexibility and reading tasks that produce higher accuracy rates.

First-level statistical analysis for all individual task runs were carried out using FSL's Improved Linear Model with local autocorrelation correction (Woolrich et al., 2001). We used a double-gamma HRF time-series convolution and set the highpass filter at 100 s for all three tasks. All task models also included six motion regressors, temporal derivatives for each regressor, and nuisance regressors that modeled out single trials identified as having excessive motion (framewise displacement greater than 0.9 mm; Siegel et al., 2014). At least 50% retention of frames after censoring was required for a run to be included (percent of frames removed for each task: inhibition $M = 7.4\%$, $SD = 8.8\%$; flexibility $M = 8.3\%$, $SD = 10\%$; reading $M = 13.7\%$, $SD = 11.2\%$). We modeled a response time regressor mean-centered across all trials for each task to decrease the likelihood that activation for our contrasts of interest were confounded by response time. This was an important confound to control for given that cingulo-opercular regions have been shown to be sensitive to response time (Neta et al., 2014; Yarkoni et al., 2009). Second-level analysis, which averaged contrast estimates over runs within subject, was carried out using a fixed effects model using FMRIB Local Analysis of Mixed Effects (FLAME; Beckmann et al., 2003; Woolrich, 2008; Woolrich et al., 2004).

The third-level group analysis was also executed using FLAME stage 1 (Beckmann et al., 2003; Woolrich, 2008; Woolrich et al., 2004), under FSL version 5.0.9. Z-statistic images were thresholded at $z > 2.5$ and coordinates and voxel size of group analysis results were obtained using the FSL version 5.0.9 Cluster tool; we report clusters of 20 voxels or more (Worsley, 2001). Brain regions are reported in MNI coordinates and identified using the Harvard-Oxford atlas in the FMRIB software and confirmed in Neurosynth (Yarkoni et al., 2011).

2.4.4. Summed mask analysis—We modeled the binarized mask analysis and *z*-thresholding after Neta and colleagues (Neta et al., 2015) and previous work from our lab that investigated common activation in brain regions during correct trials across multiple

tasks in children (Engelhardt et al., 2019). For each thresholded *z*-stat map for each task (*z* > 2.5), we assigned a value of 1 to voxels that showed significant differential activity for the error contrasts (errors vs. corrects, which includes both errors > corrects and corrects > errors); voxels that were not significant were assigned a 0. We summed the binarized maps for each task together, resulting in a single map showing voxels engaged across all three tasks, across the different combinations of two tasks, and by only one task. For visualization of the statistical maps, we projected the data onto an average inflated map using Caret software (Van Essen, 2012). Whole-brain task-specific error contrast *z*-maps, before binarization and summation, are shown in Supplementary Fig. 2. Age and task accuracy were also included in a secondary analysis of the main effect error contrasts as continuous covariates to control for any age and performance effects on error-related activation.

2.4.4. Region-of-interest (ROI) comparison—We wanted to directly assess the 11 literature-derived adult error regions (Supplementary Table 1; Neta et al., 2015) in each task of our child samples using both a distance analysis and an applied ROI analysis of our own whole brain contrasts. For the distance analysis, we used the FSL Cluster tool to identify coordinates for each cluster center within the summed mask of task-overlapping error activity, and then estimated the distances between the literature-derived adult ROIs and the child sample clusters. Distances were calculated using the following equation:

$$distance(mm) = \sqrt{(x_{child} - x_{adult})^2 + (y_{child} - y_{adult})^2 + (z_{child} - z_{adult})^2}$$

where the MNI coordinates for the child centers of activity and the adult ROIs correspond to x, y, and z.

For the applied ROI analysis, 5 mm radius spheres were created using the T1 MNI152 2 mm brain mask in FSL version 5.0.9, with the center of each sphere of the literature-based coordinates. Mean BOLD percent signal change for each ROI for each individual for the contrast of interest was also calculated using FSL and *R* version 3.3.3 (R Development Core Team, 2017). We tested for literature-derived adult ROIs that showed significantly different activations from zero between error and correct trials. Additionally, we applied the 11 literature-derived adult regions (Neta et al., 2015) to the *correct vs. baseline* and *error vs. baseline* contrasts for each task to assess the direction of the average percent signal changes for correct and error trials (inhibition *correct stops vs. baseline* and *failed stops vs. baseline*, flexibility *all correct trials vs. baseline* and *all error trials vs. baseline*, and reading *all correct trials vs. baseline* and *all error trials vs. baseline*).

2.4.5. Whole brain correlations between error activation, task accuracy, and age—We analyzed common error activation across the three tasks with third-level whole brain models that included correlates of the mean accuracy and age per person. Accuracy and age were separately entered as mean-centered correlates in a third-level group analysis for each error contrast (inhibition *correct stops vs. failed stops* contrast, flexibility *all correct vs. all error trials* contrast, and reading *all correct vs. all error trials* contrast). Within the thresholded and corrected *z*-stat maps (*z* > 2.5), we then binarized each map and summed the binarized maps together using the same steps under Summed mask analysis. We

projected the data onto an average inflated map using Caret software (Van Essen, 2012) and assessed location using the distance analysis described under *ROI comparison*.

2.5. Data and code availability

FMRI statistical analyses were conducted in FSL version 5.0.9 (www.fmrib.ox.ac.uk/fsl), as detailed in *Materials and Methods*, and task performance analyses were conducted using R version 3.3.3 (R Development Core Team, 2017; t.test and cor.test functions from the stats package). Group level thresholded and unthresholded statistical brain maps resulting from fMRI analyses across the manuscript and supplementary materials are available at the following Open Science Framework archive: https://osf.io/vqrjk

3. Results

3.1. Task performance

Descriptive statistics are provided in Table 3. Behavioral performance on all three tasks did not significantly differ by gender, with the exception of males showing better accuracy on the "Go" trials, which were not included in the neuroimaging analyses (t (211.38) = − 3.12, p = .01; corrected for multiple comparisons). We analyzed inhibition "Stop" performance and related brain activity to focus on inhibitory control, but to align with best current reporting practices for the inhibition behavioral measures (Verbruggen et al., 2019), the "Go" accuracy was 85.97% (SD = 9.74%) and the "Go" RT was 658.90 ms (SD = 81.0 ms).

Age was included as a covariate in the fMRI models to control for the effect of age on error-related activation. We also examined age in relation to error-related activation. Age was significantly positively correlated with flexibility accuracy (r = 0.45, Bonferroni corrected p < .001; Supplementary Fig. 3) and negatively correlated with flexibility RT (r = −0.54, Bonferroni corrected p < .001). Age was not significantly correlated with accuracy on the inhibition "Stop" trials (r = 0.08, un-corrected p = 0.24), likely due to the staircase design (see Materials and Methods), and was also not significantly correlated with reading accuracy (r = −0.19, Bonferroni corrected p = .44), given the small age range.

3.1. Neuroimaging results

3.1.1. Whole-brain summed masks—Significant error-related BOLD activity common across all three tasks was observed across 19 regions in the cortex (black regions in Fig. 1; Table 4), including cingulo-opercular network regions like the dACC and bilateral anterior insula. Nine subcortical regions with consistent three-task error-related activity included bilateral thalamus, bilateral hippocampus, right parahippocampal gyrus, left accumbens, right putamen, and right caudate. Error signal clusters common across all three tasks remained significant after controlling for both age and accuracy (Table 4; 28 total cortical and subcortical regions). A distinct lack of consistent error-related activity across all three tasks was seen in lateral frontal cortex.

We found additional areas of two-task overlap in children (Fig. 1; coordinates reported in Supplementary Table 2). Overlapping areas for the flexibility and inhibition tasks included the bilateral supramarginal gyrus and right posterior middle temporal gyrus, among others

(purple areas, Fig. 1). Reading and inhibition task activation overlapped in areas such as bilateral sensorimotor, bilateral superior lateral occipital cortex, and left posterior cingulate gyrus (orange areas, Fig. 1). For reading and flexibility, we found overlap in bilateral medial and lateral occipital cortex, and bilateral medial and mouth sensorimotor cortex, among others (green areas, Fig. 1).

Activity in the cingulo-opercular network had strong consistency in children, similar to prior results from the adult literature (Neta et al., 2015). Activity in fronto-parietal network regions, especially in lateral frontal cortex, was not consistent across two or three tasks in children (Fig. 1). We found a few non-overlapping frontal areas specific to each task (see Supplementary Fig. 2 and Supplementary Table 3). However, for two of the tasks (reading and inhibition), those frontal regions were small and demonstrated greater positive activity for correct relative to error trials instead of errors greater than corrects.

3.1.2. Region-of-interest (ROI) comparison—We observed good overlap with the adult error ROIs (Supplementary Table 1; Neta et al., 2015), but we also calculated the distance between the adult coordinates and the coordinates of the three task-overlapping error clusters from our child sample. Nine adult error ROIs fell within 20 mm of the centers of the child error clusters and were mainly members of the cingulo-opercular network (Fig. 1, white ROIs). The two adult error ROIs that were more than 20 mm away from the centers of task-overlapping error clusters in the child sample were the lateral frontal cortex regions (yellow regions in Fig. 1). The left dorsolateral prefrontal cortex (PFC) adult ROI was < 20 mm away from child inhibition-specific error activation in the left inferior frontal gyrus (IFG); no other task-specific child frontal activation was close to the two adult frontal ROIs.

We also applied the adult ROIs directly to the child data to test whether the adult ROIs had significant BOLD activity in children that differentiated between error and correct trials. Eight of the 11 literature-applied adult ROIs showed activation significantly different from zero for two to three tasks in our child sample; all eight also had significantly greater positive activation for errors relative to correct trials, consistent with adult activity. These eight included all of the same regions found in the distance analysis, except for the caudate ROI, which showed the same level of positive activity for both error and correct trials for the inhibition task.

3.1.3. Whole brain correlations between error activation and task accuracy— We found no reportable areas of consistent three-task overlap for the correlation between error activity and task accuracy (though note two small three-task overlap regions <8 voxels in dACC in Fig. 2). We did find multiple areas of two-task overlap where activity correlated with accuracy, such that the absolute difference in signal between correct and error trials was larger when task accuracy was higher. These overlaps included several cingulo-opercular network regions, such as the anterior cingulate, thalamus, and bilateral anterior insula (Table 5, Fig. 2). The reading task and the inhibition task also showed overlapping child error activation that correlated with accuracy in bilateral anterior insula and left thalamus (Table 5, Fig. 2). Error activation that correlated with accuracy for the reading and flexibility tasks was also found in bilateral anterior insula regions, adjacent to those found for the reading and inhibition task correlations (Table 5, Fig. 2). Additionally, there was a small area of

overlap in the left IFG for the flexibility and inhibition tasks that we do not report in Table 5 due to size (MNI coordinates: −46, +24, +16; 6 voxels; Fig. 2).

When controlling for age, most of these clusters of correlation with task accuracy survived, except the right supplementary motor region for the flexibility and inhibition tasks, and the right anterior insula region for the reading and flexibility tasks. The fronto-parietal network adult frontal ROIs were not close to any child error activation that correlated with accuracy.

3.1.4.   Whole brain correlations between error activation and age—We found no areas of three-task overlap for error signals that correlated with age, possibly due to the smaller age range (8.39 – 12.53 years) collected for the reading task, and the staircasing method used for the inhibition task. We found one small region of overlapping error activation in children that positively correlated with age for the two tasks (flexibility and inhibition) with a larger age range (7.98 – 17.20 years): an area in left medial supplementary motor cortex (MNI coordinates: −9, −6, + 61; 21 voxels; Supplementary Fig. 4). No adult error ROIs were within 20 mm of this two-task overlap region.

4.   Discussion

An understanding of error processing is intricately related to our knowledge of learning and adaptive behavior. We aimed to identify brain regions that consistently responded to task errors in a developmental sample using a multiple-task approach. We found 28 brain regions that exhibited greater positive activation for errors relative to correct trials across the three different tasks; an additional 14 brain regions showed greater activation for errors during two out of the three tasks. Our results held even when controlling for age. We found that the majority of the adult error-related regions showed a pattern of greater positive activation during errors relative to correct trials in our child sample, consistent with the adult pattern (Carp et al., 2010; Dosenbach et al., 2007; Neta et al., 2017, 2015, 2014; Wessel et al., 2012). These literature-applied, error-related adult regions have been classified as part of the brain's cingulo-opercular control network. Moreover, many cingulo-opercular brain regions were also where the error signal correlated with task performance on some of the tasks. Contrary to results from the adult literature, we did not find consistent error-differentiating signal in lateral frontal cortex. We also did not find any consistent relations with age in these regions across tasks, suggesting that the lateral frontal cortex may not be engaged for task-general error processing during childhood or adolescence (at least up to age 17).

Our results greatly extend single-task findings from previous child studies of inhibition task errors (Braet et al., 2009; Deng et al., 2017; Fitzgerald et al., 2010, 2008; Rodehacke et al., 2014; Rubia et al., 2007; Stevens et al., 2009). We demonstrate that during error processing, children engage many brain regions, in addition to the dACC, across multiple tasks, similar to adult findings (Carp et al., 2010; Dosenbach et al., 2007; Neta et al., 2017, 2015, 2014; Wessel et al., 2012). Further, we provide evidence that inhibitory control tasks, which have been widely used in the developmental error processing literature (Braet et al., 2009; Deng et al., 2017; Fitzgerald et al., 2010, 2008; Rodehacke et al., 2014; Rubia et al., 2007; Stevens et al., 2009), successfully engage a task-general set of error regions in children and remain a strong tool for studying the error processing signal. Lastly, our tasks tapped different

cognitive skills that are important for academic success: reading comprehension, inhibition, and cognitive flexibility (Berninger et al., 2017; Blair and Peters Razza, 2007). As the source and type of mistakes may differ widely across our tasks, the error processing signal consistency is all the more remarkable.

4.1. Children demonstrate mature error signaling in cingulo-opercular regions across three tasks

For a substantial number of cingulo-opercular control brain regions, children exhibited a consistent pattern of error-related activation; this was especially evident within the medial superior frontal, dACC, bilateral anterior insula, and bilateral thalamus. These regions remained significantly active for errors across all three tasks even when we controlled for age in our child sample, and in spite of the different task constraints and different behavioral relations between accuracy and age on each task. Further, these regions showed error-related activation even with the inclusion of a response time regressor. (Response time relates to activation in many cingulo-opercular regions across multiple tasks; Neta et al., 2014; Yarkoni et al., 2009.)

Our cingulo-opercular network results are consistent with adult studies (Neta et al., 2015) and single-task fMRI studies (absent of explicit feedback) in children and adolescents that show greater activation in cingulo-opercular regions for errors relative to correct trials (Deng et al., 2017; Fitzgerald et al., 2008). Several studies comparing children and adults have not found differences in error activation between age groups in cingulo-opercular control regions like the dACC and anterior insula (Braet et al., 2009; Rodehacke et al., 2014; Stevens et al., 2009). However, a few single-task studies have found age effects in the medial PFC and dACC, where adults, relative to children and adolescents, show greater differences in activation between error and correct trials (Fitzgerald et al., 2010; Velanova et al., 2008). Though we were unable to directly compare the magnitude of error-related activation between our child sample and an adult sample, our correlation with task performance in children suggests that our results are consistent, such that better task performance reflected greater differentiation between error and correct trial activity.

4.2. Children do not show consistent error-related activation in lateral frontal control regions

Unlike regions within the cingulo-opercular control network, lateral frontal brain regions, including those of the fronto-parietal control network, while significantly engaged during the tasks, failed to differentiate error trials in children across multiple tasks, whereas these regions were found to exhibit consistent error-related activation in an adult meta-analysis (Neta et al., 2015). While we did find some small *individual* task error-related activation in lateral frontal cortex, most notably for the flexibility task, demonstrating that children can potentially show frontal engagement for errors, these findings were not sizable or in a consistent location across tasks (blue regions in Supplementary Fig. 2).

We examined correlations with age to investigate maturational changes in error-related activation, which is one possible explanation for the lack of consistent lateral frontal error engagement across tasks in our child sample. However, we found no areas of three-task

overlap for error signals that correlated with age, and any sizable task-specific age-related findings were not in lateral frontal regions. To the best of our knowledge, only one other fMRI study examined correlations between age and error-related fMRI activation. Rubia and colleagues (Rubia et al., 2007) used a different inhibition task comparison (failed stop trials > all go trials) across children, adolescents, and adults (aged 10–17 and 20–42 years) and also did not find correlations between age and error activation in the lateral frontal cortex.

Additionally, task performance also did not seem to explain the inconsistent engagement of the lateral frontal cortex for errors across tasks. While we found a few relations between task accuracy and error-related activity in left lateral frontal cortex during individual tasks (flexibility and inhibition; Fig. 2), we did not find any areas of three-task overlap that related to task accuracy in lateral frontal regions.

Overall, age did not correlate with lateral frontal cortex activity in children and relations to performance in lateral frontal regions were specific to individual tasks. Therefore, we suggest that the development of lateral frontal engagement for error signaling may relate more to task-specific performance, than to age, during childhood and adolescence, at least for ages 8 to 17 years. Further, it is possible that the development of the error signal in lateral frontal cortex may continue after adolescence, as indicated by many findings that frontal lobe maturation extends into early adulthood (Blakemore and Choudhury, 2006; Giedd et al., 2009; Gogtay et al., 2004; Paus, 2005; Sowell et al., 2001).

The role of the fronto-parietal network broadly, and the lateral frontal cortex more specifically, in error signaling may be functionally different from the role of the cingulo-opercular network (Gratton et al., 2018; Neta et al., 2017, 2015). From adults, the fronto-parietal network has been proposed to support adaptive task control (Dosenbach et al., 2007, 2006). Similarly, in adults, a meta-analysis using a "slow-reveal" task paradigm found that cingulo-opercular regions were active during the response period, while bilateral fronto-parietal regions showed activity linked to pre- and post-response processing (Gratton et al., 2017). A few single-task fMRI studies in children and adolescents have examined the BOLD signal during trials before or after an error response has been made (Plessen et al., 2016; Rodehacke et al., 2014; Spinelli et al., 2011a, 2011b). In adolescents, Rodehacke and colleagues (Rodehacke et al., 2014) found that better overall task performance related to greater post-error control engagement in frontal regions. During pre-error trials relative to pre-correct trials, Spinelli and colleagues (Spinelli et al., 2011a) have found greater activation in middle frontal gyrus and angular gyrus. These studies suggest that different control networks may be involved in different points of the decision process. We hope to further address consistent fronto-parietal brain network engagement at different stages of error processing in children in future cross-task analyses.

4.3. Greater error activation in dACC and anterior insula corresponds to better performance

We found a positive correlation between task accuracy and error-related activation in core cingulo-opercular network regions across two tasks, such that the difference between the magnitude of activation for errors relative to correct trials was greater when participants demonstrated better task performance. Previous single-task studies have also found that a

"stronger" error signal is associated with improved performance in control regions during inhibition-demanding tasks (Fitzgerald et al., 2010; Rodehacke et al., 2014). Rodehacke and colleagues (Rodehacke et al., 2014) found that adolescents who committed fewer errors showed greater error-related activation in bilateral anterior insula; Fitzgerald and colleagues (Fitzgerald et al., 2010) found a similar pattern in the posterior medial frontal cortex. While the dACC and anterior insula were consistently active for error contrasts across all three tasks in our child sample, our findings suggests that the error-related signal in those regions varies on the basis of individuals' performance. This is in line with findings from adult studies showing that participants with the greatest error-related cingulo-opercular activity also made fewer errors (Neta et al., 2017).

4.5. Limitations and future directions

Our ability to fully tease apart activation during different periods of the decision process - which include pre-error, the moment of the error itself, and the post-error period when behavioral adjustments may occur - may be limited by the temporal resolution and fixed trial length design of the fMRI methodology. It is possible that the comparison of error and correct trials, which were measured within fixed windows of time (1000 ms, 4000 ms, or 8000 ms), captured cognitive processes immediately before or after an error occurred within a given error trial. Additionally, our studies did not provide performance feedback, so it is possible that brain activation during the error trials was influenced by lack of engagement. Lower error rates for some participants on the flexibility and reading tasks may have also potentially impacted error-related brain activity, since those two tasks were not designed to drive participants towards a 50% error rate like the inhibition task (see Table 3). Regardless, error-related brain activity in children was largely similar to findings from adult studies that used tasks without feedback and low error rates (Neta et al., 2015). Our task design also did not ask participants to reflect on their confidence of their decisions, which could provide insight into what might give rise to an error on a given task.

Future research could compare cross-task results with and without feedback to test whether feedback promotes greater frontal control activity. Greater sampling of older adolescents (our sample included $N = 26$ for ages 13–17, which was 11.2% of the total sample) might also help to further address questions regarding the developmental trajectory of lateral frontal cortex activation that differentiates error and correct trials. Further, examination of error-signaling temporal profiles common across tasks in children would provide additional insight into the role of error regions during different periods of the decision process and across maturation (e.g., Buzzell et al., 2017; Neta et al., 2015). Lastly, future and ongoing longitudinal event-related fMRI studies that cross a broader, or younger, developmental range could specifically analyze the development of error-related activation in frontal control regions from childhood into adulthood.

4.6. Conclusions

This study aimed to identify brain areas with consistent error signals across multiple fMRI tasks in a large sample of children and adolescents, expanding a literature limited to using single inhibitory control tasks. We found that participants show greater fMRI activation for errors relative to correct trials in cingulo-opercular brain areas, consistent with error regions

found in an adult meta-analysis. However, unlike adults, our child sample did not show consistent error-related activation in lateral frontal regions or relations with age across multiple tasks. Our findings suggest that lateral frontal regions may differentiate mature from immature error processing, in line with extant literature that indicates later functional and structural maturation of the frontal lobe. Characterizing consistent error-related brain regions during typical development sets a framework for understanding error processing in clinical developmental populations with poor behavioral regulation of control, such as attention-deficit/hyperactivity disorder.

Supplementary Material

Refer to Web version on PubMed Central for supplementary material.

Acknowledgements

References

Beckmann CF, Jenkinson M, Smith SM, 2003. General multilevel linear modeling for group analysis in FMRI. Neuroimage 20, 1052–1063. 10.1016/S1053-8119(03)00435-X. [PubMed: 14568475]

Berninger V, Abbott R, Cook CR, Nagy W, 2017. Relationships of attention and executive functions to oral language, reading, and writing skills and systems in middle childhood and early adolescence. J. Learn. Disabil 50, 434–449. 10.1177/0022219415617167. [PubMed: 26746315]

Blair C, Peters Razza R, 2007. Relating effortful control, executive function, and false belief understanding to emerging math and literacy ability in kindergarten. Child Dev. 78, 647–663. [PubMed: 17381795]

Blakemore SJ, Choudhury S, 2006. Development of the adolescent brain: implications for executive function and social cognition. J. Child Psychol. Psychiatry Allied Discip 47, 296–312. 10.1111/j.1469-7610.2006.01611.x.

Braet W, Johnson KA, Tobin CT, Acheson R, Bellgrove MA, Robert-son IH, Garavan H, 2009. Functional developmental changes underlying response inhibition and error-detection processes. Neuropsychologia 47, 3143–3151. 10.1016/j.neuropsychologia.2009.07.018. [PubMed: 19651151]

Buzzell GA, Richards JE, White LK, Barker TV, Pine DS, Fox NA, 2017. Development of the error-monitoring system from ages 9–35: Unique insight provided by MRI-constrained source localization of EEG. Neuroimage 157, 13–26. 10.1016/j.neuroimage.2017.05.045. [PubMed: 28549796]

Carp J, Kim K, Taylor SF, Fitzgerald KD, Weissman DH, 2010. Conditional differences in mean reaction time explain effects of response congruency, but not accuracy, on posterior medial frontal cortex activity. Front. Hum. Neurosci 4, 231. 10.3389/fnhum.2010.00231. [PubMed: 21212836]

Carrasco M, Harbin SM, Nienhuis JK, Fitzgerald KD, Gehring WJ, Hanna GL, 2013. Increased error-related brain activity in youth with obsessive-compulsive disorder and unaffected siblings. Depress. Anxiety 30, 39–46. [PubMed: 23225541]
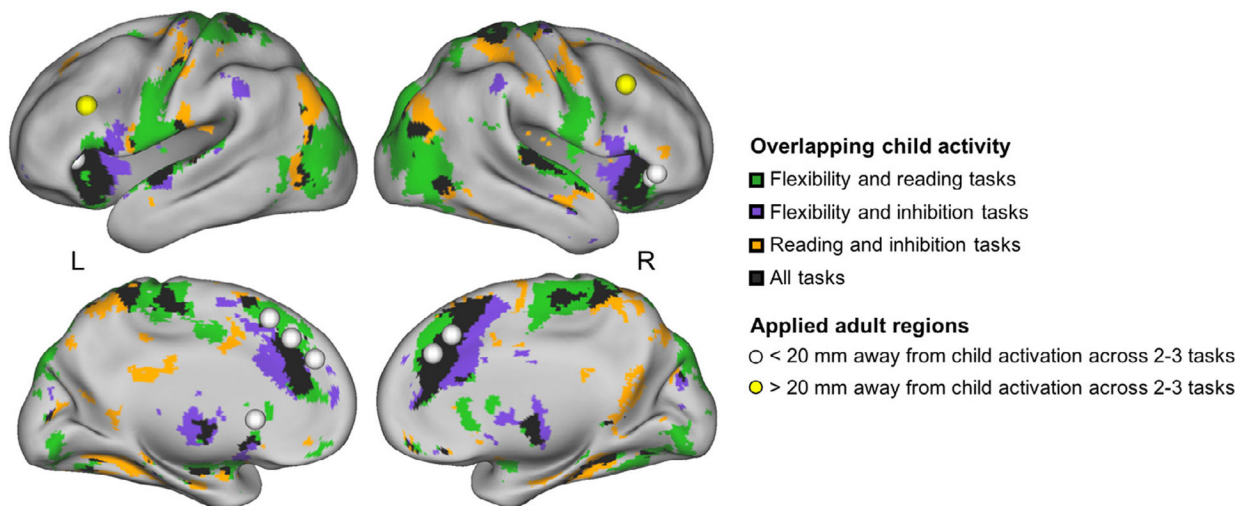
Congdon E, Mumford JA, Cohen JR, Galvan A, Canli T, Poldrack RA, 2012. Measurement and reliability of response inhibition. Front. Psychol 3, 1–10. 10.3389/fpsyg.2012.00037. [PubMed: 22279440]

Deng W, Rolls ET, Ji X, Robbins TW, Banaschewski T, Bokde ALW, Bromberg U, Buechel C, Desrivières S, Conrod P, Flor H, Frouin V, Gallinat J, Garavan H, Gowland P, Heinz A, Ittermann B, Martinot JL, Lemaitre H, Nees F, Orfanos DP, Poustka L, Smolka MN, Walter H, Whelan R, Schumann G, Feng J, 2017. Separate neural systems for behavioral change and for emotional responses to failure during behavioral inhibition. Hum. Brain Mapp 38, 3527–3537. 10.1002/hbm.23607. [PubMed: 28429498]

Dosenbach NUF, Fair DA, Cohen AL, Schlaggar BL, Petersen SE, 2008. A dual-networks architecture of top-down control. Trends Cogn. Sci 12, 99–105. 10.1016/j.tics.2008.01.001. [PubMed: 18262825]

Dosenbach NUF, Fair DA, Miezin FM, Cohen AL, Wenger KK, Dosenbach RAT, Fox MD, Snyder AZ, Vincent JL, Raichle ME, Schlaggar BL, Petersen SE, 2007. Distinct brain networks for adaptive and stable task control in humans. Proc. Natl. Acad. Sci. U. S. A 104, 11073–11078. 10.1073/pnas.0704320104. [PubMed: 17576922]

Dosenbach NUF, Visscher KM, Palmer ED, Miezin FM, Wenger KK, Kang HC, Burgund ED, Grimes AL, Schlaggar BL, Petersen SE, 2006. A core system for the implementation of task sets. Neuron 50, 799–812. 10.1016/j.neuron.2006.04.031. [PubMed: 16731517]

Engelhardt LE, Harden KP, Tucker-Drob EM, Church JA, 2019. The neural architecture of executive functions is established by middle childhood. Neuroimage 185, 479–489. 10.1016/j.neuroimage.2018.10.024. [PubMed: 30312810]

Fitzgerald KD, Perkins SC, Angstadt M, Johnson T, Stern ER, Welsh RC, Taylor SF, 2010. The development of performance-monitoring function in the posterior medial frontal cortex. Neuroimage 49, 3463–3473. 10.1016/j.neuroimage.2009.11.004. [PubMed: 19913101]

Fitzgerald KD, Zbrozek CD, Welsh RC, Britton JC, Liberzon I, Taylor SF, 2008. Pilot study of response inhibition and error processing in the posterior medial prefrontal cortex in healthy youth. J. Child Psychol. Psychiatry Allied Discip 49, 986–994. 10.1111/j.1469-7610.2008.01906.x.

Giedd JN, Lalonde FM, Celano MJ, White SL, Wallace GL, Lee NR, Lenroot RK, 2009. Anatomical brain magnetic resonance imaging of typically developing children and adolescents. J. Am. Acad. Child Adolesc. Psychiatry 48, 465–470. 10.1097/CHI.0b013e31819f2715. [PubMed: 19395901]

Gogtay N, Giedd JN, Lusk L, Hayashi KM, Greenstein D, Vaituzis AC, Nugent Iii TF, Herman DH, Clasen LS, Toga AW, Rapoport JL, Thompson PM, 2004. Dynamic mapping of human cortical development during childhood through early adulthood. Proc. Natl. Acad. Sci. U. S. A 101, 8174–8179. [PubMed: 15148381]

Gratton C, Neta M, Sun H, Ploran EJ, Schlaggar BL, Wheeler ME, Petersen SE, Nelson SM, 2017. Distinct stages of moment-to-moment processing in the cinguloopercular and frontoparietal networks. Cereb. Cortex 27, 2403–2417. 10.1093/cercor/bhw092. [PubMed: 27095824]

Gratton C, Sun H, Petersen SE, 2018. Control networks and hubs. Psychophysiology 55, 1–18. 10.1111/psyp.13032.

Greve DN, Fischl B, 2009. Accurate and robust brain image alignment using boundary based registration. Neuroimage 48, 63–72. [PubMed: 19573611]

Harden KP, Tucker-Drob EM, Tackett JL, 2013. The Texas twin project. Twin Res. Hum. Genet 16, 385–390. 10.1017/thg.2012.97. [PubMed: 23111007]

Holroyd CB, Coles MGH, 2002. The neural basis of human error processing: rein-forcement learning, dopamine, and the error-related negativity. Psychol. Rev 109, 679–709. 10.1037/0033-295X.109.4.679. [PubMed: 12374324]

Jenkinson M, Bannister P, Brady M, Smith S, 2002. Improved optimization for the robust and accurate linear registration and motion correction of brain images. Neuroimage 17, 825–841. [PubMed: 12377157]

Jenkinson M, Smith S, 2001. A global optimisation method for robust affine registration of brain images. Med. Image Anal 5, 143–156. 10.1016/S1361-8415(01)00036-6. [PubMed: 11516708]

Johnson KA, Kelly SP, Bellgrove MA, Barry E, Cox M, Gill M, Robert-son IH, 2007. Response variability in attention deficit hyperactivity disorder: evidence for neuropsychological
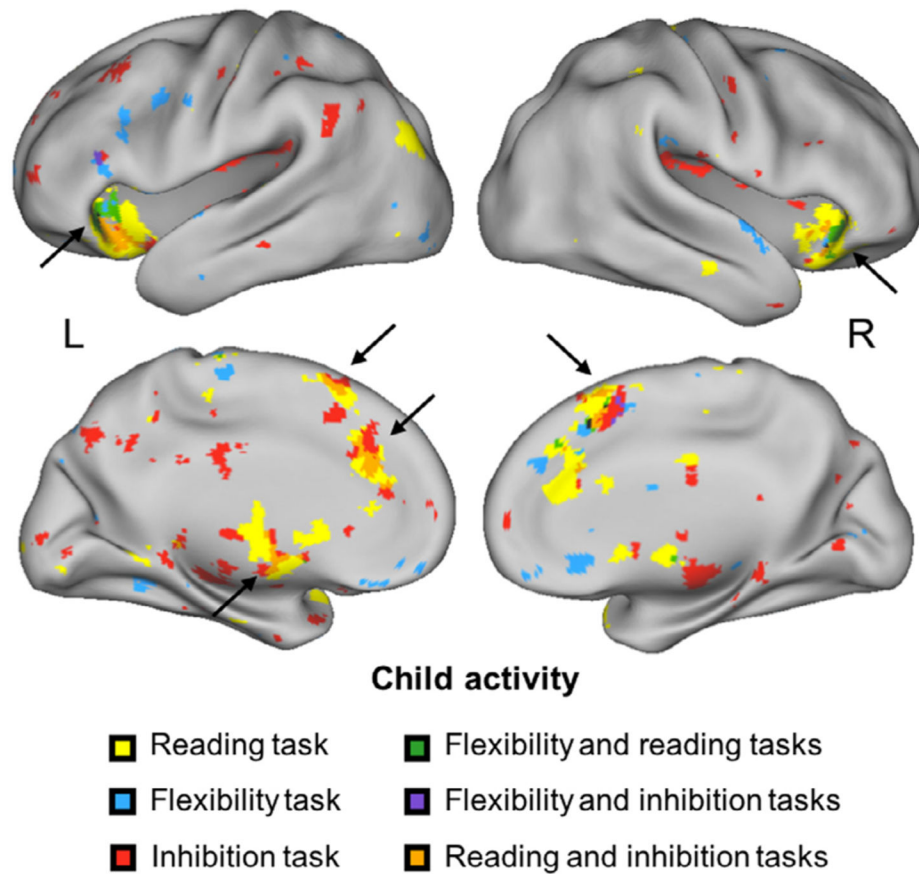

heterogeneity. Neuropsychologia 45, 630–638. 10.1016/j.neuropsychologia.2006.03.034. [PubMed: 17157885]

Kessler RC, Amminger GP, Aguilar-Gaxiola S, Alonso J, Lee S, Bedirhan Ustun T, 2007. Age of onset of mental disorders: a review of recent literature. Curr. Opin. Psychiatry 20, 359–364. [PubMed: 17551351]

Luna B, Padmanabhan A, O'Hearn K, 2010. What has fMRI told us about the development of cognitive control through adolescence? Brain Cogn. 72, 101–113. 10.1016/j.bandc.2009.08.005. [PubMed: 19765880]

Merikangas KR, He JP, Burstein M, Swanson SA, Avenevoli S, Cui L, Benjet C, Georgiades K, Swendsen J, 2010. Lifetime prevalence of mental disorders in U.S. adolescents: results from the national comorbidity survey replication-adolescent supplement (NCS-A). J. Am. Acad. Child Adolesc. Psychiatry 49, 980–989. 10.1016/j.jaac.2010.05.017. [PubMed: 20855043]

Meyler A, Keller TA, Cherkassky VL, Lee D, Hoeft F, Whitfield-Gabrieli S, Gabrieli JDE, Just MA, 2007. Brain activation during sentence comprehension among good and poor readers. Cereb. Cortex 17, 2780–2787. 10.1093/cercor/bhm006. [PubMed: 17317678]

Mullane JC, Corkum PV, Klein RM, McLaughlin E, 2009. Interference control in children with and without ADHD: a systematic review of flanker and simon task performance. Child Neuropsychol 15, 321–342. 10.1080/09297040802348028. [PubMed: 18850349]

Neta M, Miezin XM, Nelson SM, Dubis JW, Dosenbach NUF, Schlaggar BL, Petersen SE, 2015. Spatial and temporal characteristics of error-related activity in the human brain. J. Neurosci 35, 253–266. 10.1523/JNEUROSCI.1313-14.2015. [PubMed: 25568119]

Neta M, Nelson SM, Petersen SE, 2017. Dorsal anterior cingulate, medial superior frontal cortex, and anterior insula show performance reporting-related late task control signals. Cereb. Cortex 27, 2154–2165. 10.1093/cercor/bhw053. [PubMed: 26972752]

Neta M, Schlaggar BL, Petersen SE, 2014. Separable responses to error, ambiguity, and reaction time in cingulo-opercular task control regions. Neuroimage 99, 59–68. 10.1016/j.neuroimage.2014.05.053. [PubMed: 24887509]

Nugiel T, Roe MA, Taylor WP, Cirino PT, Vaughn SR, Fletcher JM, Juranek J, Church JA, 2019. Brain activity in struggling readers before intervention relates to future reading gains. Cortex 111, 286–302. 10.1016/j.cortex.2018.11.009. [PubMed: 30557815]

Paus T, 2005. Mapping brain maturation and cognitive development during adolescence. Trends Cogn. Sci 9, 60–68. 10.1016/j.tics.2004.12.008. [PubMed: 15668098]

Peirce JW, 2007. PsychoPy–psychophysics software in Python. J. Neurosci. Methods 162, 681.

Plessen KJ, Allen EA, Eichele H, van Wageningen H, Høvik MF, Sørensen L, Worren MK, Hugdahl K, Eichele T, 2016. Reduced error signalling in medicationnaive children with ADHD: associations with behavioural variability and post-error adaptations. J. Psychiatry Neurosci 41, 77–87. 10.1503/jpn.140353. [PubMed: 26441332]

Power JD, Petersen SE, 2013. Control-related systems in the human brain. Curr. Opin. Neurobiol 23, 223–228. 10.1016/j.conb.2012.12.009. [PubMed: 23347645]

R Development Core Team. R: a language and environment for statistical computing, 2017.

Reuter M, Rosas HD, Fischl B, 2010. Highly accurate inverse consistent registration: a robust approach. Neuroimage 53, 1181–1196. 10.1016/j.neuroimage.2010.07.020. [PubMed: 20637289]

Rodehacke S, Mennigen E, Müller KU, Ripke S, Jacob MJ, Hübner T, Schmidt DHK, Goschke T, Smolka MN, 2014. Interindividual differences in mid-adolescents in error monitoring and post-error adjustment. PLoS One 9, e88957. 10.1371/journal.pone.0088957. [PubMed: 24558455]

Roe MA, Martinez JE, Mumford JA, Taylor WP, Cirino PT, Fletcher JM, Juranek J, Church JA, 2018. Control engagement during sentence and inhibition fMRI tasks in children with reading difficulties. Cereb. Cortex 28, 3697–3710. 10.1093/cercor/bhy170. [PubMed: 30060152]

Rubia K, Smith AB, Taylor E, Brammer M, 2007. Linear age-correlated functional development of right inferior fronto-striato-cerebellar networks during response inhibition and anterior cingulate during error-related processes. Hum. Brain Mapp 28, 1163–1177. 10.1002/hbm.20347. [PubMed: 17538951]

Rubia K, Smith AB, Woolley J, Nosarti C, Heyman I, Taylor E, Brammer M, 2006. Progressive increase of frontostriatal brain activation from childhood to adulthood during event-related tasks of cognitive control. Hum. Brain Mapp 27, 973–993. 10.1002/hbm.20237. [PubMed: 16683265]

Schachar RJ, Chen S, Logan GD, Ornstein TJ, Crosbie J, Ickowicz A, Pakulak A, 2004. Evidence for an error monitoring deficit in attention deficit hyperactivity disorder. J. Abnorm. Child Psychol 32, 285–293. [PubMed: 15228177]

Siegel JS, Power JD, Dubis JW, Vogel AC, Church JA, Schlaggar BL, Petersen SE, 2014. Statistical improvements in functional magnetic resonance imaging analyses produced by censoring high-motion data points. Hum. Brain Mapp 35, 1981–1996. 10.1002/hbm.22307. [PubMed: 23861343]

Sowell ER, Thompson PM, Tessner KD, Toga AW, 2001. Mapping continued brain growth and gray matter density reduction in dorsal frontal cortex: inverse relationships during postadolescent brain maturation. J. Neurosci 21, 8819–8829. [PubMed: 11698594]

Spinelli S, Joel S, Nelson TE, Vasa RA, Pekar JJ, Mostofsky SH, 2011a. Different neural patterns are associated with trials preceding inhibitory errors in children with and without attention-deficit/hyperactivity disorder. J. Am. Acad. Child Adolesc. Psychiatry 50, 705–715. [PubMed: 21703498]

Spinelli S, Vasa RA, Joel S, Nelson TE, Pekar JJ, Mostofsky SH, 2011b. Variability in post-error behavioral adjustment is associated with functional abnormalities in the temporal cortex in children with ADHD. J. Child Psychol. Psychiatry Allied Discip 52, 808–816. 10.1111/j.1469-7610.2010.02356.x.

Steele VR, Anderson NE, Claus ED, Bernat EM, Rao V, Assaf M, Pearlson GD, Calhoun VD, Kiehl KA, 2016. Neuroimaging measures of error-processing: Extracting reliable signals from event-related potentials and functional magnetic resonance imaging. Neuroimage 132, 247–260. 10.1016/j.neuroimage.2016.02.046. [PubMed: 26908319]

Stevens MC, Kiehl KA, Pearlson GD, Calhoun VD, 2009. Brain network dynamics during error commission. Hum. Brain Mapp 30, 24–37. 10.1002/hbm.20478. [PubMed: 17979124]

Tamnes CK, Walhovd KB, Torstveit M, Sells VT, Fjell AM, 2013. Performance monitoring in children and adolescents: a review of developmental changes in the error-related negativity and brain maturation. Dev. Cogn. Neurosci 6, 1–13. 10.1016/j.dcn.2013.05.001. [PubMed: 23777674]

Van Essen DC, 2012. Cortical cartography and Caret software. Neuroimage 62, 757–764. [PubMed: 22062192]

Velanova K, Wheeler ME, Luna B, 2008. Maturational changes in anterior cingulate and frontoparietal recruitment support the development of error processing and inhibitory control. Cereb. Cortex 18, 2505–2522. 10.1093/cercor/bhn012. [PubMed: 18281300]

Verbruggen F, Aron AR, Band GPH, Beste C, Bissett PG, Brockett AT, Brown JW, Chamberlain SR, Chambers CD, Colonius H, Colzato LS, Corneil BD, Coxon JP, Dupuis A, Eagle DM, Garavan H, Greenhouse I, Heathcote A, Huster RJ, Jahfari S, Kenemans JL, Leunissen I, Li CSR, Logan GD, Matzke D, Morein-Zamir S, Murthy A, Paré M, Poldrack RA, Ridderinkhof KR, Robbins TW, Roesch M, Rubia K, Schachar RJ, Schall JD, Stock AK, Swann NC, Thakkar KN, Van Der Molen MW, Vermeylen L, Vink M, Wessel JR, Whelan R, Zandbelt BB, Boehler CN, 2019. A consensus guide to capturing the ability to inhibit actions and impulsive behaviors in the stop-signal task. Elife 8, e46323. 10.7554/eLife.46323. [PubMed: 31033438]

Verbruggen F, Logan GD, 2008. Response inhibition in the stop-signal paradigm. Trends Cogn. Sci 12, 418–424. 10.1016/j.tics.2008.07.005. [PubMed: 18799345]

Wessel JR, Aron AR, 2017. On the globality of motor suppression: unexpected events and their influence on behavior and cognition. Neuron 93, 259–280. 10.1016/j.neuron.2016.12.013. [PubMed: 28103476]

Wessel JR, Danielmeier C, Bruce Morton J, Ullsperger M, 2012. Surprise and error: common neuronal architecture for the processing of errors and novelty. J. Neurosci 32, 7528–7537. 10.1523/JNEUROSCI.6352-11.2012. [PubMed: 22649231]

Woolrich M, 2008. Robust group analysis using outlier inference. Neuroimage 41, 286–301. 10.1016/j.neuroimage.2008.02.042. [PubMed: 18407525]

Woolrich MW, Behrens TEJ, Beckmann CF, Jenkinson M, Smith SM, 2004. Multilevel linear modelling for FMRI group analysis using Bayesian inference. Neuroimage 21, 1732–1747. 10.1016/j.neuroimage.2003.12.023. [PubMed: 15050594]

Woolrich MW, Ripley BD, Brady M, Smith SM, 2001. Temporal autocorrelation in univariate linear modeling of FMRI data. Neuroimage 14, 1370–1386. [PubMed: 11707093]

Worsley KJ, 2001. Functional MRI: an introduction to methods. Oxford Medical Publications.

Yarkoni T, Barch DM, Gray JR, Conturo TE, Braver TS, 2009. BOLD correlates of trial-by-trial reaction time variability in gray and white matter: a multi-study fMRI analysis. PLoS One 4, e4257. 10.1371/journal.pone.0004257. [PubMed: 19165335]

Yarkoni T, Poldrack RA, Nichols TE, Van Essen DC, Wager TD, 2011. Large scale automated synthesis of human functional neuroimaging data. Nat. Methods 8, 665–670. [PubMed: 21706013]

Overlapping child activity

- ■ Flexibility and reading tasks
- ■ Flexibility and inhibition tasks
- ■ Reading and inhibition tasks
- ■ All tasks

Applied adult regions

- ○ < 20 mm away from child activation across 2-3 tasks
- ● > 20 mm away from child activation across 2-3 tasks

Fig. 1. Child error activity across multiple tasks overlaid with literature-applied adult ROIs.
Selected child error contrasts were the inhibition *correct stops vs. failed stops*, the flexibility *all correct vs. all error trials,* and the reading *all correct vs. all error trials*. Nine of eleven adult regions of interest (ROIs; from Neta et al., 2015) were within 20 mm of cluster activation for three-task overlapping child error contrasts (white spheres); the lateral frontal lobe ROIs (yellow spheres) are the exceptions.
ROI = region-of-interest.

Child activity

☐ Reading task ☐ Flexibility and reading tasks
☐ Flexibility task ☐ Flexibility and inhibition tasks
☐ Inhibition task ☐ Reading and inhibition tasks

Fig. 2. Overlapping child error activity correlated with task accuracy.
Error contrasts for the inhibition, flexibility, and reading tasks were correlated with mean accuracy. Arrows indicate activation in regions that correlate with accuracy for at least two of the tasks (see Table 5 for coordinates). Selected error contrasts were the inhibition *correct stops vs. failed stops*, the flexibility *all correct vs. all error trials*, and the reading *all correct vs. all error trials*. Before binarizing and summing the masks for each contrast, maps were thresholded at $z > 2.5$.

Table 1

Participant demographics.

	Twin Study (Total unique N = 77)	Executive Function Study (Total unique N = 28)	Reading Study (Total unique N = 127)
Tasks (N)			
Flexibility	71	24	-
Inhibition	75	25	118
Reading	-	-	118
Mean age (SD)	10.47 y (1.45 y)	12.59 y (2.57 y)	10.24 y (0.87 y)
Age range	7.98–14.44 y	8.77–17.20 y	8.22–12.53 y
Gender (N)			
Female	42 (54.5 %)	10 (35.7 %)	67 (52.7 %)
Male	35 (45.5 %)	18 (64.3 %)	60 (47.3 %)
Race/ethnicity (N)			
Hispanic	22 (28.6 %)	5 (17.9 %)	48 (37.8 %)
Non-Hispanic white	36 (46.7 %)	20 (71.4 %)	47 (37.0 %)
Black	7 (9.1 %)	2 (7.1 %)	26 (20.5 %)
Native American	0 (0.0 %)	0 (0.0 %)	1 (0.8 %)
Asian	8 (10.4 %)	0 (0.0 %)	0 (0.0 %)
Multiracial	4 (5.2 %)	1 (3.6 %)	3 (2.4 %)

Notes. Two participants in the Reading Study did not report race/ethnicity. SD = standard deviation; y = years.

Table 2

Design details for the three tasks used in the analysis.

	Inhibition Task	Flexibility Task	Reading Task
Contrast	Correct stops vs. failed stops	All correct vs. all error trials	All correct vs. all error trials
Stimuli	Arrows, red X	Shapes	Written sentences
Input modality	Visual	Visual	Visual
Response modality	Button	Button	Button
Participants	218	95	118
Runs per participant	1–2	1–2	1–3
Trials per run	32 stop trials	37 target trials	32 sentence trials
TR	2000 ms	2000 ms	2000 ms
Stimulus ITI range	0–7000 ms	0–8000 ms	0–8000 ms
Stimulus duration	1000 ms	4000 ms	8000 ms
Scanner	3T	3T	3T
Design type	Event-related	Event-related	Event-related

Notes. Also see Supplementary Fig. 1.

Table 3

Descriptive statistics for scanner task performance.

Task	Performance measure	Description	n	M	SD	Range
Flexibility	Accuracy	Proportion correct	95	85.76 %	9.89 %	55.41–98.65 %
	RT	Mean RT	95	1057 ms	171.86 ms	579.80–1409.80 ms
	Errors	Mean total number of error trials	95	10.75 trials	7.93 trials	1–34 trials
Inhibition	Stop accuracy	Proportion correct, stop trials	218	55.36 %	4.37 %	37.50–70.31 %
	Inhibition RT	Stop signal RT	218	230.30 ms	63.36 ms	99.44–463.40 ms
	Inhibition SSD	Stop signal delay	218	412.7 ms	103.10 ms	100.00–675.00 ms
	Stop errors	Mean total number of failed stop trials	218	22.10 trials	7.41 trials	10–39 trials
Reading	Accuracy	Proportion correct	118	83.38 %	11.96 %	50.0–98.96 %
	RT	Mean RT	118	3998 ms	835.33 ms	1725.18–6234.9 ms
	Errors	Mean total number of error trials	118	13.66 trials	8.67 trials	2–45 trials

Notes. Exclusionary criteria for task performance required, per run, > 50% flexibility task accuracy, > 50% inhibition "Go" accuracy, > 50 ms SSRT, and > 50% reading task accuracy, but at least 1 error across all usable runs. RT = response time; SSD = stop signal delay.

Table 4

Overlapping centers of error-related activity common across all three tasks in children.

Cluster size	Region	MNI Coordinates		
		x	y	z
1650	dACC	+2	+25	+37
964	L anterior insula	−36	+17	−1
855	R anterior insula	+38	+19	−1
329	L posterior STG	−61	−16	+2
252	R posterior STG	+66	−20	+6
66	R anterior STG	+59	−2	−9
76	L inferior lateral occipital	−46	−71	+1
317	R inferior lateral occipital	+44	−70	+11
97	L superior lateral occipital	−33	−78	+31
24	L medial superior parietal	−12	−66	+59
36	L central opercular	−57	−19	+16
22	R precentral gyrus	+36	−17	+66
32	R postcentral gyrus	+29	−26	+67
1744	R medial precuneus	+3	−41	+61
25	R medial frontal	+7	+46	−12
48	R precuneus	+5	−78	+42
21	R cuneal cortex	+2	−81	+25
23	R posterior cingulate	+13	−48	+6
21	Intracalcarine/lingual cortex	0	−84	+3
55	L thalamus	−2	−25	−2
32	L thalamus	−6	−11	+4
33	R thalamus	+8	−10	+3
168	R parahippocampal gyrus	+32	−37	−11
90	L hippocampus	−20	−14	−18
54	R hippocampus	+19	−11	−17
24	L accumbens	−7	+8	−6
32	R caudate	+10	+4	+12
28	R putamen	+24	+11	−1

Notes. The FSL *cluster* command was applied to the summed activation map to determine cluster sizes and coordinates. We report cortical and subcortical clusters comprising 20 voxels or more. L = left; R = right; dACC = dorsal anterior cingulate cortex; STG = superior temporal gyrus.

Table 5

Two-task overlapping centers of error-related activity related to task accuracy.

Tasks	Cluster size	Region	MNI Coordinates		
			x	y	z
Flexibility + Inhibition	23	R supplementary motor	+5	+9	+50
Reading + Inhibition	279	L anterior insula	−33	+15	−10
Reading + Inhibition	43	R anterior insula	+33	+18	−5
Reading + Inhibition	165	medial superior frontal (dorsal)	0	+16	+53
Reading + Inhibition	97	L anterior cingulate	−6	+25	+32
Reading + Inhibition	27	L thalamus	−9	−8	+6
Reading + Flexibility	95	L anterior insula	−33	+22	0
Reading + Flexibility	72	R anterior insula	+35	+23	0

Notes. The FSL *cluster* command was applied to the summed activation map to determine cluster sizes and coordinates. We report cortical and subcortical clusters comprising 20 voxels or more. L = left; R = right.